https://ntrs.nasa.gov/search.jsp?R=19940030744 2020-06-16T12:55:14+00:00Z

6-20-94
E8916

NASA Technical Memorandum 106625
AIAA–94–3259

Experimental Results of Hydrogen Slosh in a 62 Cubic Foot (1750 Liter) Tank

Matthew E. Moran, Nancy B. McNelis, and Maureen T. Kudlac
Lewis Research Center
Cleveland, Ohio

Mark S. Haberbusch
Ohio Aerospace Institute
Brook Park, Ohio

and

George A. Satornino
Sverdrup Technology
Sandusky, Ohio

Prepared for the
30th Joint Propulsion Conference
cosponsored by AIAA, ASME, SAE, and ASEE
Indianapolis, Indiana, June 27–29, 1994

National Aeronautics and
Space Administration

EXPERIMENTAL RESULTS OF HYDROGEN SLOSH IN A 62 CUBIC FOOT (1750 LITER) TANK

Matthew E. Moran, Nancy B. McNelis, and Maureen T. Kudlac
National Aeronautics and Space Administration
Lewis Research Center
Cleveland, Ohio 44135
and
Mark S. Haberbusch
Ohio Aerospace Institute
Brook Park, Ohio 44142
and
George A. Satornino
Sverdrup Technology, Inc.
Sandusky, Ohio 44870

Abstract

Extensive slosh testing with liquid and slush hydrogen was conducted in a 62 cubic foot spherical tank to characterize the thermodynamic response of the system under normal gravity conditions. Slosh frequency and amplitude, pressurant type, ramp pressure, and ullage volume were parametrically varied to assess the effect of each of these parameters on the tank pressure and fluid/wall temperatures. A total of 91 liquid hydrogen, and 62 slush hydrogen slosh tests were completed. Both closed tank tests and expulsions during sloshing were performed. This report presents and discusses highlights of the liquid hydrogen closed tank results in detail, and introduces some general trends for the slush hydrogen tests. Summary comparisons between liquid and slush hydrogen slosh results are also presented.

Introduction

A critical concern for the National Aero-Space Plane (NASP) development is the thermodynamic response of the slush/liquid hydrogen propellant tank under sloshing conditions. Sloshing is expected to occur during vehicle taxi, takeoff, and flight maneuvers. Fluid motion produced during these operations can circulate subcooled hydrogen near the liquid-vapor interface resulting in increased condensation and corresponding pressure collapse. Conversely, liquid contact on hot tank walls caused by sloshing can result in rapid vaporization and subsequent rapid pressure rise. It is essential that both scenarios are predictable and controllable in order to insure safe and reliable operation of the NASP vehicle.

Experimental data in the open literature on the thermodynamic effects of liquid hydrogen slosh is quite limited. Open literature data on slush hydrogen slosh is nonexistent. Yet the availability of such data is crucial to characterizing the underlying phenomena driving the thermodynamic response of a liquid or slush hydrogen propellant tank. The evolution of accurate simulation capabilities will also rely heavily on experimental databases for verification. These capabilities support not only the NASP program, but potentially all launch/space vehicles utilizing subcritical or subcooled cryogenic propellants. Furthermore, the significance of thermodynamic slosh effects become ever more important as future mission profiles result in greater bulk fluid motion (e.g. longer coasts under low gravity conditions, more abrupt vehicle maneuvers, and partial rotations of the propellant tanks). Under these situations, complex fluid dynamics of the liquid cryogen primarily dictate the transient thermodynamic response within the propellant tank. Therefore, computational fluid dynamic techniques, coupled to interfacial heat and mass transfer algorithms, will likely be necessary to accurately predict pressure and temperature conditions. To the authors' knowledge, this analytical capability does not presently exist.

In order to investigate slosh and other operational issues associated with slush hydrogen handling aboard the NASP, a test program was undertaken at the NASA Lewis Research Center's K-site facility located at the Plum Brook Station. The tests were performed in a spherical tank containing slush management and measurement components. Results of the liquid hydrogen slosh tests, and general trends with slush hydrogen, are the focus of this paper. The test series was funded by the United States NASP program, Joint Propulsion Office, Wright-Patterson Air Force Base.

Experimental Rig Description

The K-site test facility is designed for large scale testing with liquid hydrogen. Slush hydrogen production and test capability was added to the facility in 1990. K-site is believed to be the only currently operational slush hydrogen facility in the United States. For this test series, a three shift per day operation was conducted, with research tests conducted during two of the shifts.

Copyright © 1994 by the American Institute of Aeronautics and Astronautics, Inc. No copyright is asserted in the United States under Title 17, U.S. Code. The U.S. Government has a royalty-free license to exercise all rights under the copyright claimed herein for Governmental purposes. All other rights are reserved by the copyright owner.

Operation, control and data acquisition is performed remotely in a control room located approximately 540 feet from the test building. Cryogen and gas facility storage/delivery capacities are: 26,000 gal. LH_2; 24,500 gal. LN_2; 250,000 scf GHe and GN_2 each; and 140,000 scf GH_2. Pressurant gas can be thermally conditioned using steam, liquid nitrogen, and/or liquid hydrogen heat exchangers. Subatmospheric conditions within the test tank are achieved through the low pressure vent system using a single-stage vacuum pump. A sketch of the test tank internals and instrumentation used for the slosh tests is shown in Fig. 1.

Test Tank and Vacuum Chamber

The aluminum test tank is mounted inside a 25 foot diameter stainless steel vacuum chamber which maintains a nominal vacuum range of 10^{-6} torr during testing (10^{-7} torr empty) via four diffusion pumps upstream of four more vacuum pumps. Some of the K-site test crew standing in, and in front of, the vacuum chamber are shown in Fig. 2. The test tank is visible near the center of the photograph, mounted from four flexure straps. Around the perimeter of the vacuum chamber are the bolts used to secure the 20 foot diameter chamber door prior to pulling a vacuum. At the far left of the photo are the hinges which support the chamber door. The grating inside the vacuum chamber provides access to the tank and does not interfere with the sloshing motion.

Slosh is produced by a shaker mechanism capable of six inches of total displacement at a frequency of one Hertz. The sloshing system shaft penetration at the rear of the vacuum chamber is shown in Fig. 3. The shaft translates along a roller support (near the center of the photograph), and mounts to the test tank support structure at the far left. Also visible at the extreme left of the photograph is one of the stainless steel flexure straps.

The test tank is shown in Fig. 4 from the front of the chamber, near the opening. Visible in the photograph is the support structure and tank externals. The tank lid is constructed of stainless steel, while the remainder of the tank is aluminum. Steady state environmental heat leak into the tank is 0.3 Btu/s. At the middle left of the photo, on the upper hemisphere of the tank, is the view port and video camera assembly protected by a long cylindrical cannister. The video camera records the internal tank conditions through the viewing port, which is approximately 60 degrees above the tank midline, and 40 degrees left of the sloshing system shaft axis, from an observation point directly at the chamber opening.

Instrumentation and Data Acquisition

Test tank instrumentation includes (refer to Fig. 1): silicon diodes for temperature sensing on the tank walls and internally; thermocouples for some fluid stream temperatures; pressure transducers; liquid level probe; vapor-liquid point sensors; measured mass flowrate of pressurant and propellant streams; and a densimeter for solid fraction measurement of slush hydrogen.

The internal silicon diodes are mounted to an instrument tree, and provide an indication of both axial and radial temperature distributions in the tank. External tank diodes are mounted directly to the tank wall. Accuracy of the diodes at liquid hydrogen temperatures is approximately ±1°R. Silicon diodes are also utilized as vapor-liquid sensors by using overcurrent to induce self heating. Type E thermocouples provide fluid stream and other system temperatures at ±2°R.

Liquid level is measured by a capacitance-type probe which was specially designed in-house for use in liquid and slush hydrogen. The readings from the probe are compensated for pressure and temperature (due to changes in fluid dielectric constant) in the data acquisition software. *In situ* accuracy of the probe was found to be nominally ± 0.25 inches when compared to the vapor-liquid point sensors.

Pressurant mass flowrate is measured using orifices coupled to temperature and pressure data with a calculated uncertainty of ±0.00012 lbm/s. Strain gauge type pressure transducers measure various system pressures to within ±0.5% full scale.

The data acquisition and display system is controlled by a local minicomputer with 512 data channels available; recorded data is eventually uploaded to a mainframe system located at Lewis for data reduction. Nominal sample rates are once per second, with the capability of ten times per second. Several displays throughout the control room show operational and research data in real time during testing.

Test Procedure

For the closed tank slosh tests (i.e. no pressurant inflow nor propellant outflow during sloshing) the test tank is filled to the desired level with either liquid or slush hydrogen, and then vented to approximately 1 atm if necessary. The pressurization gas temperature is then preconditioned using the liquid hydrogen and/or liquid nitrogen heat exchanger(s). If the test fluid is slush hydrogen, the propeller mixer is turned on to promote uniform solid fraction, and the propellant density is measured after the mixer is off. With the temperature of the pressurization gas conditioned, the tank is pressurized with either hydrogen or helium to the desired tank pressure. After stopping pressurant flow and closing the vent valve, shaking is initiated at the preset frequency, and

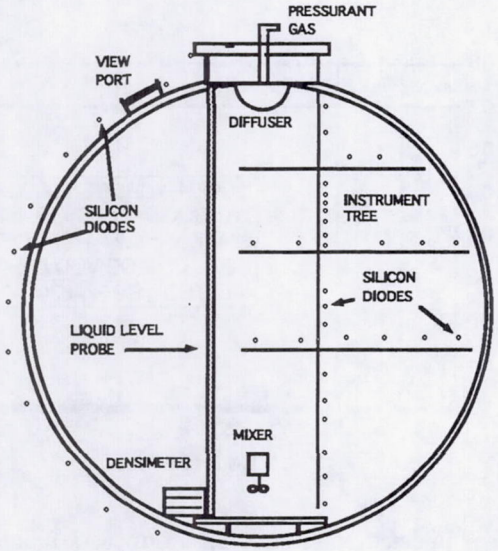

Fig. 1. Sketch of the test tank internals and instrumentation

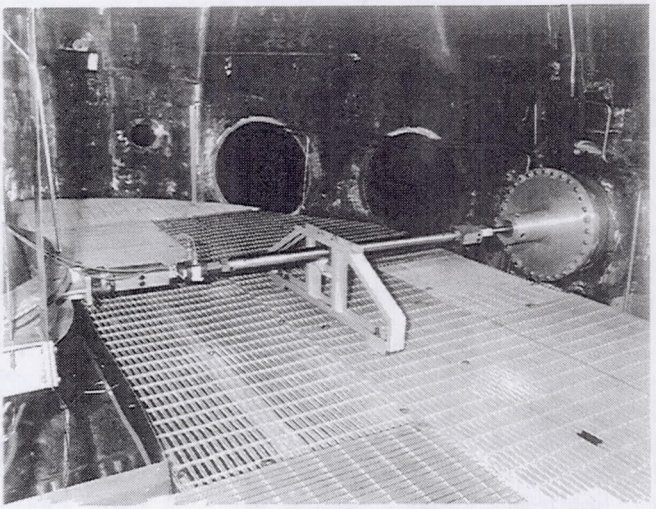

Fig. 3. Photograph of the shaker shaft

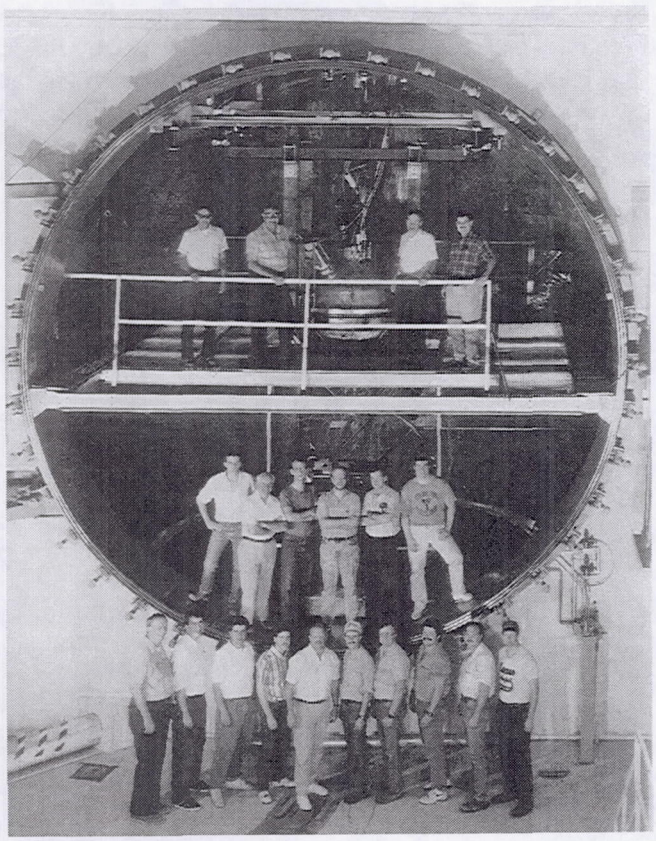

Fig. 2. Photograph of the vacuum chamber

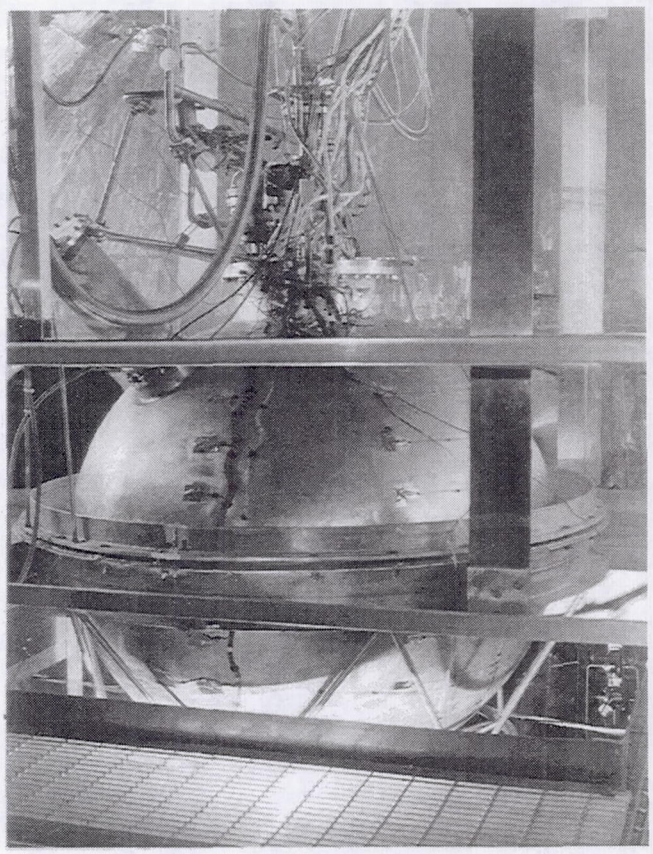

Fig. 4. Photograph of the test tank installed in the vacuum chamber

the amplitude is increased to the desired value. The test amplitude is reached in approximately 10 to 30 seconds. Shaking is maintained for a minimum of two minutes after reaching the desired frequency and amplitude at which time the test is terminated.

Results and Discussion

In a typical slosh test, the tank pressure is ramped from near atmospheric pressure to either 20 or 35 psia, with either gaseous hydrogen or helium pressurant. A brief hold phase follows where the tank pressure is held constant, after which the pressurization valve is closed and shaking is initiated. The amplitude is gradually increased to the final setting in approximately 10 to 30 seconds. For many of the large amplitude tests (i.e. 0.74 Hz, ±1.5 inches) a sudden change in the slope of the pressure curve is evident when the desired amplitude is reached. An example of the pressure response for one such test is shown in Fig. 5. Tank pressure response for closed tank slosh tests with non-heated walls ranged from complete pressure collapse to a mild pressure rise, depending on experimental conditions.

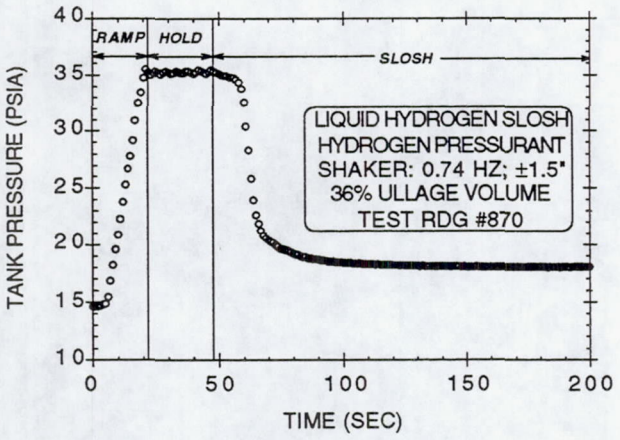

Fig. 5. Pressure response for a liquid hydrogen slosh test.

For the closed tank tests, the pressurant mass flow is nonzero through the ramp and hold phases, and goes to zero when the tank is locked up (closed) prior to initiating slosh. The pressurant injection mass flow as a function of time for the same test is given in Fig. 6.

Figure 7 illustrates the thermal response inside the tank during the same slosh test. Fluid temperatures are given as a function of vertical height, where the internal top of the tank is approximately 57 inches. Straight lines are drawn between sensor points (denoted by plot symbols) to aid interpretation, but do not necessarily imply linear temperature distributions. Initial fluid temperature distribution prior to ramp pressurization is given by the circle symbols and solid line. Liquid level within the tank is also indicated in Fig. 7.

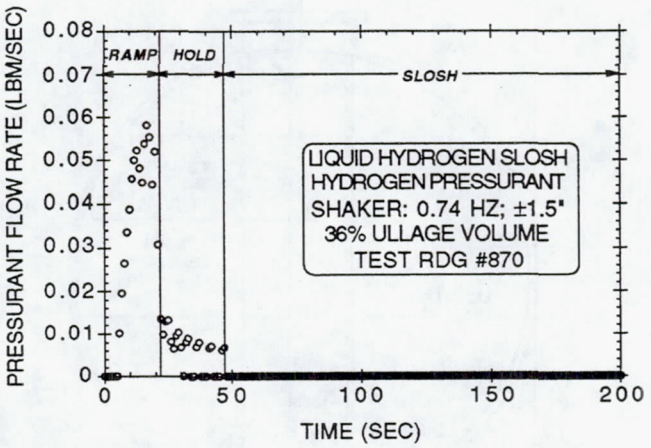

Fig. 6. Injected pressurant mass flow as a function of time for a liquid hydrogen slosh test.

Initially, large thermal stratification generally exists in the ullage. Fluid temperatures after the ramp pressurization phase are denoted by the square symbols and the large-dash line. A temperature rise in the ullage is evident as a result of the addition of pressurant gas, and the subsequent increase in tank pressure. Final fluid temperatures following slosh are shown with the triangle symbols and short-dash line. The temperature profile after slosh depends on the experimental conditions, ranging from a high degree of ullage thermal stratification to near equilibrium conditions.

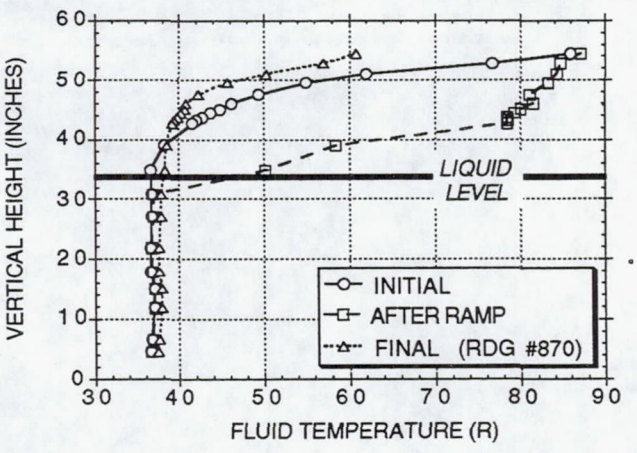

Fig. 7. Fluid temperature distributions (liquid and vapor): initially; after ramp pressurization; and after sloshing ("final").

Tank wall temperatures are given as a function of height for the same test in Fig. 8, where the external height of the tank is 58 inches. The same symbol and line conventions used for the fluid temperature plot is also used for the tank wall temperature plot. Initially, the tank wall tends to mirror the temperature distribution trends evident in the fluid region. Some of the energy added to the system during ramp pressurization is transferred to the wall as evidenced by a slight increase in wall temperatures for the "after ramp" case. The final wall temperature profile depends on the experimental conditions, although in all cases the upper portions of the wall remain thermally stratified due to the mass of the lid and the numerous piping and electrical penetrations (i.e. heat leak paths).

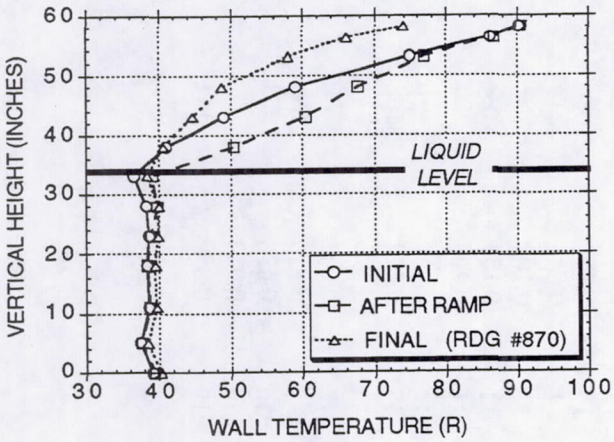

Fig. 8. Tank wall temperature distributions: initially; after ramp pressurization; and after sloshing ("final").

Summary test conditions for selected closed tank liquid hydrogen slosh tests are shown in Table I. Missing values (denoted by "-") indicate data that was not properly recorded for that test run; "n/a" is listed for parameters that do not pertain to that particular test (i.e. pressure rise occurred during slosh). The table is sorted by the following test parameters (in order of priority) to facilitate interpretation of trends: shaker frequency and amplitude setting; pressurant type; ramp pressure; and ullage volume.

The ullage volume shown in the table indicates the percentage of the total tank volume which is occupied by gas. Pressurant temperature is a time-weighted average (i.e. not weighted for mass flowrate); instantaneous values fluctuated less than 25°R during the ramp and hold pressurization phases unless otherwise noted. The pressure collapse values are a measure of the degree of saturation in the tank resulting from the slosh, and are given by,

$$\%\text{Collapse} = \frac{P_r - P_{min}}{P_r - P_{init}}\,(100\%) \qquad (1)$$

where: P_r = ramp pressure
P_{min} = minimum pressure during slosh
P_{init} = initial pressure before ramp

Therefore, a collapse value of 100% would indicate saturation conditions (at the initial tank pressure) exist after sloshing. The maximum slope of the pressure curve (i.e. dP/dt) is also given in the table, where a positive value indicates pressure rise. Finally, the test reading numbers are assigned by the data acquisition system in historical order and are unique to a specific test run.

Frequency and Amplitude

Two frequency and amplitude shaker settings were chosen for this test series: one in the stable slosh region, and one in the unstable (near resonance) region. To establish these regions, the natural frequency for a spherical tank partially filled with liquid was found from (Stofan and Armstead)[1],

$$\omega_n = \frac{1}{2\pi}\sqrt{\frac{\lambda g}{R}} \qquad (2)$$

where: ω_n = natural frequency
g = gravitational acceleration
R = tank radius
λ = empirical constant based on liquid height and tank radius (see Table II)

Using the calculated natural frequency, stability boundaries for both planar and nonplanar motion can be estimated from another experimentally derived relation (Sumner)[2]:

$$\left(\frac{\omega_0}{\omega_n}\right)^2 = K_1 + K_2\left(\frac{X_0}{2R}\right)^{\frac{2}{3}} \qquad (3)$$

where: ω_0 = excitation frequency
X_0 = excitation amplitude
$K_{1,2}$ = empirical constants

(see Fig. 9)

Table I. Selected Test Conditions for Liquid Hydrogen Slosh Tests

Freq& Ampl (Hz; ±in)	Pressurant Type	Ullage Volume (%total)	Initial Pressure (psia)	Ramp Pressure (psia)	Ramp Time (s)	Ramp Pressurant Added (lbm)	Hold Time (s)	Total Pressurant Added (lbm)	Pressurant Temperature (°R)	Min Pressure During Slosh (psia)	Pressure Collapse (%)	Max dP/dt During Slosh (psi/s)	Test Rdg#
0.95; 0.5	He	17	14.1	20.6	5	0.099	1	0.110	233	n/a	n/a	0.07	187
0.95; 0.5	He	31	14.1	19.8	40	0.137	0	0.137	171	n/a	n/a	0.03	197
0.95; 0.5	He	51	-	19.9	-	-	10	-	172	n/a	n/a	0.03	200
0.95; 0.5	He	33	-	34.7	-	-	-	-	170*	n/a	n/a	0.03	160
0.95; 0.5	H_2	17	14.5	20.1	3	0.057	15	0.075	222	18.4	30	-0.07	302
0.95; 0.5	H_2	28	14.0	19.8	6	0.115	18	0.153	221	18.1	29	-0.08	261
0.95; 0.5	H_2	49	14.7	20.7	8	0.236	4	0.264	212	18.9	30	-0.19	370
0.95; 0.5	H_2	13	14.6	36.1	13	0.314	14	0.382	81	22.1	65	-1.11	877
0.95; 0.5	H_2	17	14.2	35.0	14	0.273	36	0.353	193	26.7	40	-0.25	235
0.95; 0.5	H_2	31	14.4	34.7	17	0.369	16	0.452	234	28.6	30	-0.27	246
0.95; 0.5	H_2	33	15.4	35.4	13	0.625	28	0.816	71	29.5	29	-0.11	869
0.95; 0.5	H_2	49	14.2	34.7	23	0.587	13	0.685	249†	28.6	30	-0.29	242
0.95; 0.5	H_2	51	14.9	35.7	14	0.920	16	1.052	76	31.2	21	-0.08	886
0.74; 1.5	He	17	14.2	19.5	4	0.075	1	0.083	238	n/a	n/a	0.11	190
0.74; 1.5	H_2	17	14.1	20.2	3	0.068	11	0.100	169	16.1	67	-0.26	303
0.74; 1.5	H_2	28	14.1	19.9	5	0.106	11	0.134	199	15.9	69	-0.39	260
0.74; 1.5	H_2	54	14.0	19.8	8	0.169	11	0.208	200	16.1	64	-0.11	263
0.74; 1.5	H_2	13	15.3	35.8	12	0.301	13	0.366	72	18.9	80	-1.04	892
0.74; 1.5	H_2	15	14.6	35.7	14	0.342	17	0.417	76	18.1	83	-1.57	878
0.74; 1.5	H_2	19	14.2	34.9	14	0.260	24	0.326	224	19.8	73	-1.06	236
0.74; 1.5	H_2	31	15.1	35.7	38	0.535	13	0.641	78†	18.2	83	-2.49	893
0.74; 1.5	H_2	36	14.6	35.5	14	0.634	27	0.813	74	18.0	84	-2.55	870
0.74; 1.5	H_2	49	14.5	34.7	20	0.495	16	0.598	263	21.0	68	-0.52	243
0.74; 1.5	H_2	51	14.8	35.4	14	0.818	14	0.973	83†	19.4	77	-0.48	895
0.74; 1.5	H_2	54	14.7	35.7	15	0.781	19	0.899	111†	19.4	78	-0.34	887

* Logbook estimate

† Pressurant temperature range greater than 25°R, but less than 55°R

\- Data not recorded

n/a Not applicable to test response

Table II. Values for Constant in Eqn. (2)[1]

h/2R	$\sqrt{\lambda}$
0.1	1.0573
0.2	1.0938
0.3	1.1370
0.4	1.1893
0.5	1.2540
0.6	1.3376
0.8	1.4528
0.9	1.9770

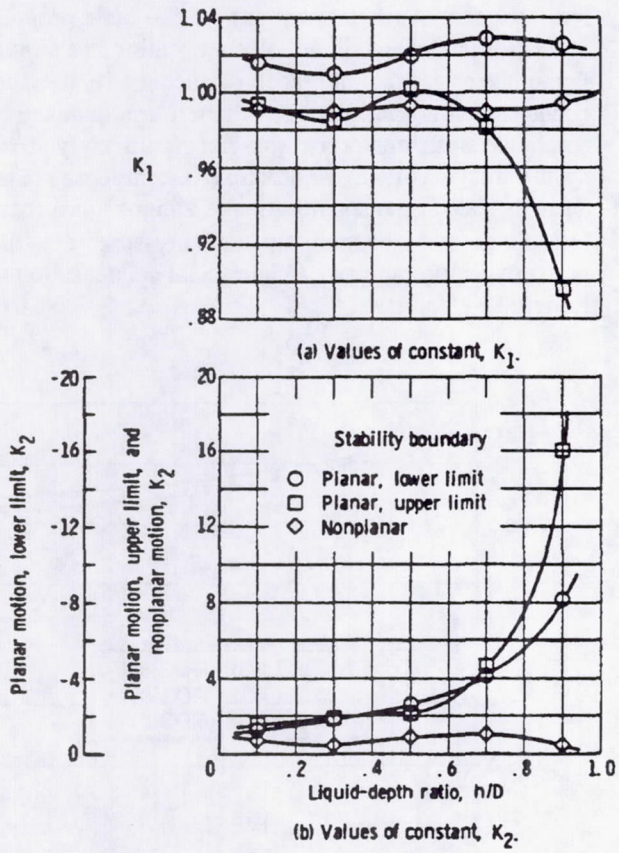

Fig. 9. Values of constants for eqn. (3)[2]

Equations (2) and (3) were used to construct slosh stability maps for the test tank as a function of slosh amplitude and frequency, and ullage volume (i.e. liquid height). Using these maps, a setting of 0.95 Hz, ±0.5 inches was chosen for stable slosh, and 0.74 Hz, ±1.5 inches was chosen for unstable slosh. These settings provide the desired liquid response for ullage volumes between 15% and 50%, as indicated in Fig.10. The nonplanar stability limit establishes the boundary where rotary slosh becomes unstable (to the left of the limit line). Similarly, the upper and lower planar stability limits define the region where wave motion parallel to the excitation axis becomes unstable (within the limit lines). Superposition of these regions defines areas of stable and unstable slosh, where stability is defined as a steady state harmonic slosh response.

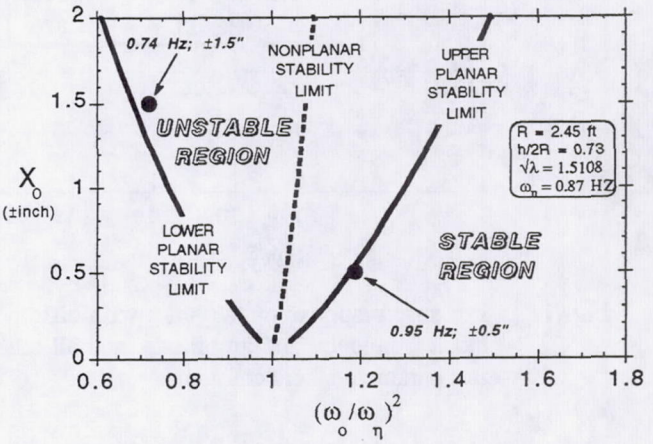

(a) 15% ullage

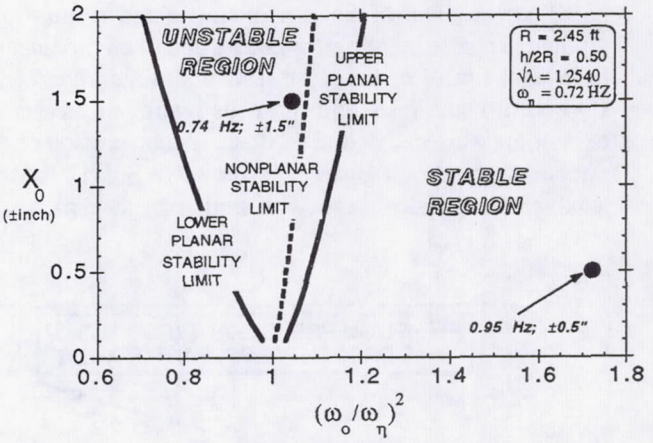

(b) 50% ullage

Fig. 10. Slosh stability map for two ullage volumes; and chosen shaker settings.

Considerably less pressure decay is observed for the low amplitude slosh setting (0.95 Hz, ±0.5") as compared to the high amplitude setting (0.74 Hz, ±1.5"). An example of the difference in pressure response is shown in Fig. 11 for two tests with all other test parameters held constant. Examination of the fluid temperature data and video recordings indicate that the high amplitude, unstable slosh causes significant circulation of the subcooled bulk

liquid toward the interface. This circulation results in increased condensation at the interface, and a correspondingly larger pressure drop in the ullage for this slosh setting.

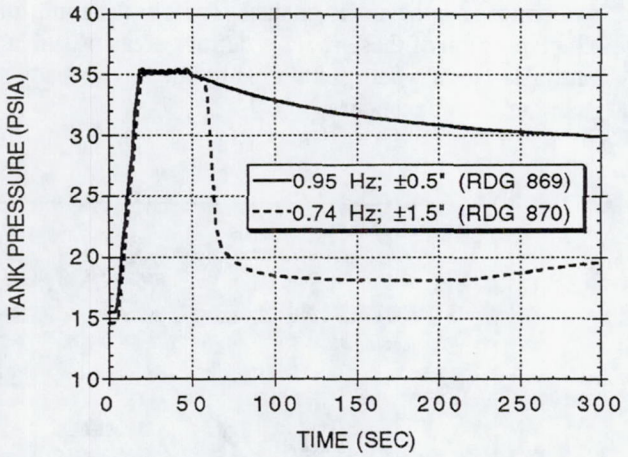

Fig. 11. Pressure response of two tests with different slosh frequency and amplitude, and all other test parameters held constant.

Helium Pressurant

The presence of helium in the ullage results in a gradual pressure increase (primarily due to environmental heat leak) for all of the slosh tests with liquid hydrogen. By contrast, the tests with gaseous hydrogen pressurant exhibit pressure decay during slosh. A comparison of the effects of pressurant gas type is shown in Fig. 12 for two small amplitude slosh tests with similar parameters.

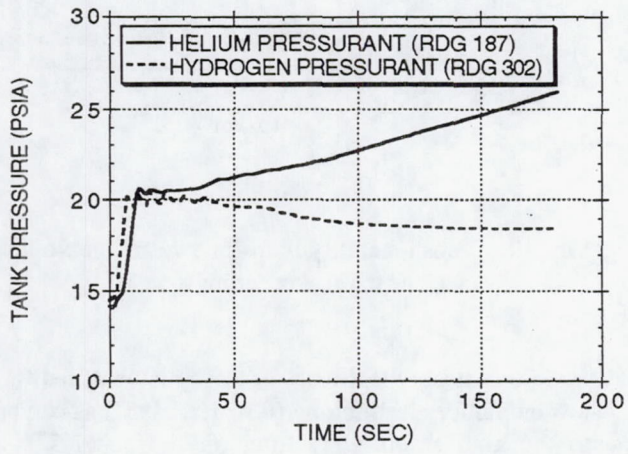

Fig. 12. Pressure response of one test using helium ramp pressurization, and the other using gaseous hydrogen, with all other parameters similar.

Note that no purges were performed between helium ramp tests. Therefore, the initial quantity of gaseous helium in the ullage is generally unknown. For this reason, comparisons of pressure response among helium pressurant tests must be made cautiously; general comparisons between helium and gaseous hydrogen pressurant tests, however, are valid. Also, note that average pressurant temperatures vary greatly among some tests depending on the conditioning heat exchanger(s) used (e.g. liquid nitrogen or liquid nitrogen and liquid hydrogen).

Ullage Volume

No consistent trend can be extracted relating ullage volume to pressure response for the high amplitude liquid hydrogen slosh tests. For the low amplitude (stable) slosh, however, it appears that the final tank pressure is directly proportional to the ullage volume, as demonstrated in Fig. 13. Temperature data and video indicates that much less mixing of the bulk propellant occurs for the low amplitude slosh, resulting in a stratified liquid layer near the interface. Consequently, the rate of condensation at the interface is much less than the high amplitude slosh, and probably is not significantly affected by the ullage volume. Therefore, the highest pressure decay is seen at the smallest ullage volume since there is less ullage mass to maintain tank pressure (i.e. ullage pressure is more sensitive to interfacial condensation with lower ullage volume).

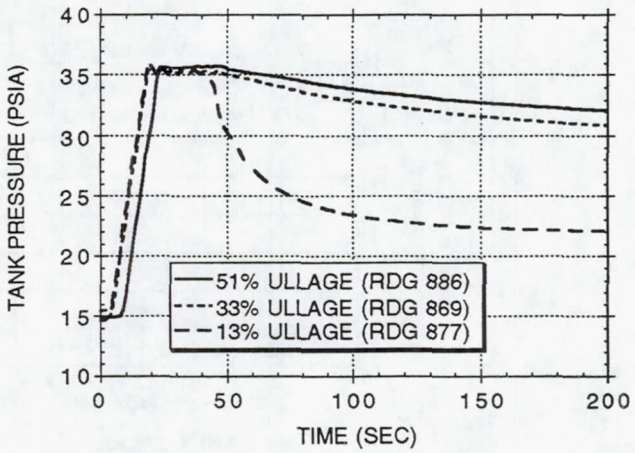

Fig. 13. Pressure response of three low amplitude slosh tests with different ullage volumes, and all other test parameters held constant.

Slush Hydrogen

Slush hydrogen exhibits greater pressure decay/collapse than liquid hydrogen under similar slosh

conditions due to the greater subcooling available. This subcooling results in much greater interfacial condensation rates, and subsequently greater pressure decay/collapse. Figure 14 demonstrates this trend for two slosh tests with similar test conditions.

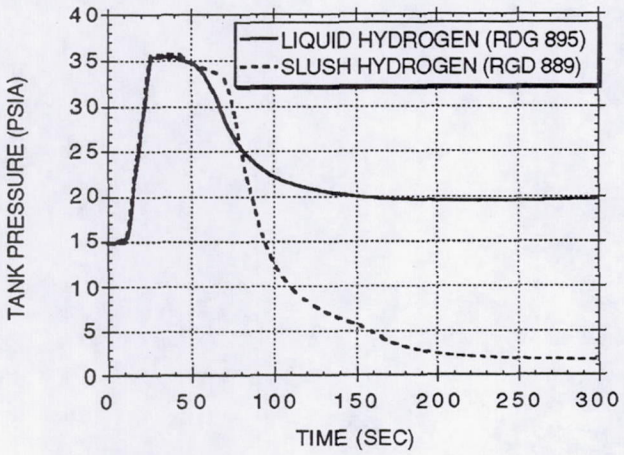

Fig. 14. Comparison of pressure response for liquid versus slush hydrogen.

The same trends previously described for liquid hydrogen slosh (i.e. frequency and amplitude, pressurant type, and ullage volume) are observed for the slush hydrogen tests. In addition, some unique features are evident from the video and sensor data for the slush hydrogen tests. For instance, the solid particles tend to settle quickly to the bottom of the tank. In fact, a completely homogeneous mixture of liquid and solid particles was never achieved, even with the large amplitude sloshing and the propellant mixer on. Consequently, a layer of thermally stratified liquid hydrogen was prevalent in the upper portion of the propellant; while the solid particles mixed with liquid hydrogen at constant triple point temperature remained in the lower portion of the propellant. During expulsions, this separation of liquid and slush hydrogen resulted in solid particles being expelled from the tank rather quickly as the fill/drain valve was opened. As reported in earlier studies[3], no significant handling problems were encountered. However, greater care was required in the chilldown of transfer lines/components and the test tank to retain an acceptable solid fraction. The solid fraction for all slush slosh tests ranged from approximately 30% to 50%, with a mean value of 37%.

Concluding Remarks

Results from this test series have shed new light on how various parameters affect the thermodynamic response of a liquid/slush hydrogen tank undergoing slosh. Tank pressure - and propellant, ullage, and wall temperatures - have been characterized for a variety of test conditions in both stable and unstable slosh regimes. Information on pressurant mass and flowrate requirements for pressurizing static tanks containing liquid and slush hydrogen has been added to the existing database. Pressure collapse magnitude and rate has also been recorded.

The nature of the slosh excitation frequency and amplitude dramatically effects the tank thermodynamic response. Sloshing near the natural frequency of the tank-liquid system (i.e. in the unstable region) can result in severe ullage collapse; whereas, slosh in the stable regions generally has little effect on the pressure response of the tank. Equations (2) and (3), coupled with estimates of the anticipated excitation frequencies and amplitudes for a given vehicle and mission profile, can be utilized to map the slosh stability regions for a spherical tank. Results of this test series can then be used to give a qualitative idea of what the thermodynamic tank response will be. Thus, corrective action (e.g. baffles, modified mission profile, additional pressurant, etc.) can be undertaken in the design stage to mitigate potential slosh problems. These test results may also have limited application to other tank geometries (see Refs. 4 and 5 for calculation of natural frequency for cylindrical and circular crossection tankage).

Other parameters found to affect the tank thermodynamic response include pressurant type and ullage volume. The effects of these secondary parameters have been characterized under a variety of conditions. Finally, significant differences in the pressure response between liquid and slush hydrogen has been observed, as well as some peculiarities associated with the handling of slush hydrogen.

Data collected and analyzed from this test program provides an empirical database with which to gauge the importance of potential thermodynamic slosh response on future launch/space vehicles. Perhaps a more vital use for this data, however, is the validation of analytical/numerical simulation methods. The coupling of computational fluid dynamic techniques to accurate thermodynamic algorithms will undoubtedly be required to adequately predict sloshing effects for a wider variety of tank geometries, hardware, and conditions.

References

1. Stofan, A.J., and Armstead, A.L., "Analytical and Experimental Investigation of Forces and Frequencies Resulting from Liquid Sloshing in a Spherical Tank", NASA TN D-1281, July, 1962.

2. Sumner, I.E., Experimental Investigation of Stability Boundaries for Planar and Nonplanar Sloshing in Spherical Tanks", NASA TN D-3210, January, 1966.

3. Hardy, T.L., and Whalen, M.V., "Technology Issues Associated With Using Densified Hydrogen for Space Vehicles", NASA TM-105642, 28th Joint Propulsion Conference, AIAA-92-3079, July, 1992.

4. Budiansky, B., "Sloshing of Liquids in Circular Canals and Spherical Tanks", Journal of the Aero/Space Sciences, Vol. 27, No. 3, pp 161-173, March, 1960.

5. McCarty, J.L., and Stephens, D.G., "Investigation of the Natural Frequencies of Fluids in Spherical and Cylindrical Tanks", NASA TN D-252, 1961.

REPORT DOCUMENTATION PAGE

Form Approved
OMB No. 0704-0188

Public reporting burden for this collection of information is estimated to average 1 hour per response, including the time for reviewing instructions, searching existing data sources, gathering and maintaining the data needed, and completing and reviewing the collection of information. Send comments regarding this burden estimate or any other aspect of this collection of information, including suggestions for reducing this burden, to Washington Headquarters Services, Directorate for Information Operations and Reports, 1215 Jefferson Davis Highway, Suite 1204, Arlington, VA 22202-4302, and to the Office of Management and Budget, Paperwork Reduction Project (0704-0188), Washington, DC 20503.

1. AGENCY USE ONLY (*Leave blank*)	2. REPORT DATE	3. REPORT TYPE AND DATES COVERED
	June 1994	Technical Memorandum

4. TITLE AND SUBTITLE

Experimental Results of Hydrogen Slosh in a 62 Cubic Foot (1750 Liter) Tank

5. FUNDING NUMBERS

WU–763–22–21

6. AUTHOR(S)

Matthew E. Moran, Nancy B. McNelis, Maureen T. Kudlac,
Mark S. Haberbusch, and George A. Satornino

7. PERFORMING ORGANIZATION NAME(S) AND ADDRESS(ES)

National Aeronautics and Space Administration
Lewis Research Center
Cleveland, Ohio 44135–3191

8. PERFORMING ORGANIZATION REPORT NUMBER

E–8916

9. SPONSORING/MONITORING AGENCY NAME(S) AND ADDRESS(ES)

National Aeronautics and Space Administration
Washington, D.C. 20546–0001

10. SPONSORING/MONITORING AGENCY REPORT NUMBER

NASA TM–106625
AIAA–94–3259

11. SUPPLEMENTARY NOTES

Prepared for the 30th Joint Propulsion Conference cosponsored by AIAA, ASME, SAE, and ASEE, Indianapolis, Indiana, June 27–29, 1994. Matthew E. Moran, Nancy B. McNelis, and Maureen T. Kudlac, NASA Lewis Research Center; George A. Satornino, Ohio Aerospace Institute, 22800 Cedar Point Road, Brook Park, Ohio 44142; and Mark S. Haberbusch, Sverdrup Technology, 6100 Columbus Ave., Sandusky, Ohio 44870 (work funded by NASA Contract NAS3–25517). Responsible person, Matthew E. Moran, organization code 5340, (216) 433–7525.

12a. DISTRIBUTION/AVAILABILITY STATEMENT

Unclassified - Unlimited
Subject Category 34

12b. DISTRIBUTION CODE

13. ABSTRACT ***(Maximum 200 words)***

Extensive slosh testing with liquid and slush hydrogen was conducted in a 62 cubic foot spherical tank to characterize the thermodynamic response of the system under normal gravity conditions. Slosh frequency and amplitude, pressurant type, ramp pressure, and ullage volume were parametrically varied to assess the effect of each of these parameters on the tank pressure and fluid/wall temperatures. A total of 91 liquid hydrogen, and 62 slush hydrogen slosh tests were completed. Both closed tank tests and expulsions during sloshing were performed. This report presents and discusses highlights of the liquid hydrogen closed tank results in detail, and introduces some general trends for the slush hydrogen tests. Summary comparisons between liquid and slush hydrogen slosh results are also presented.

14. SUBJECT TERMS	15. NUMBER OF PAGES
Cryogenics; Liquid hydrogen; Sloshing; Slush hydrogen; Liquid propulsion	12
	16. PRICE CODE: A03

17. SECURITY CLASSIFICATION OF REPORT	18. SECURITY CLASSIFICATION OF THIS PAGE	19. SECURITY CLASSIFICATION OF ABSTRACT	20. LIMITATION OF ABSTRACT
Unclassified	Unclassified	Unclassified	